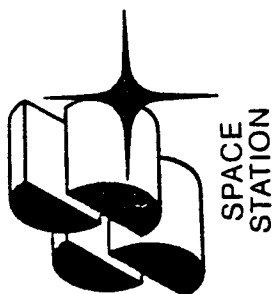


N 87 - 22721



# **Structural/Control Interaction (Payload Pointing and Micro-g)**

**Presented to**

**NASA / MSFC**

**Workshop on Structural Dynamics**

**and**

**Control Interaction of Flexible Structures**

**April 22, 1986**

**Presented by C. R. Larson  
(213) 922-2031**

PRECEDING PAGE BLANK NOT FILMED

## CHART 1.

On Space Station there are two important customer accommodation requirements: payload pointing and migro-g. A simulation model was developed to evaluate the system capability to meet the requirements. The pointing requirement of a payload is not defined but is expected to be around one arc second. The acceleration requirement for a material processing or life science experiment is  $1 \times 10^{-3}$  G's.

# Structural/Control Interaction Objectives

---



- EVALUATE THE CAPABILITY OF A TYPICAL SPACE STATION PAYLOAD TO MEET ITS POINTING REQUIREMENT (POINTING REQUIREMENT MAY BE ONE ARC SEC)
- DETERMINE IF THE G-LEVEL REQUIREMENT OF  $1 \times 10^{-5}$  G CAN BE PROVIDED FOR MATERIAL PROCESSING EXPERIMENTS



Rockwell International  
Space Station Systems Division

## CHART 2

Two simulation models were developed. One with a coarse pointing control system and one with a fine pointing control system. The agenda will address both simulations. The coarse simulation is running and the results from the simulation will be discussed. The fine is in the beginning stage of development and will only be briefly mentioned.

# Structural/Control Interaction Agenda

---



- SIMULATION MODEL
  - COARSE CONTROLLER
    - DEFINITION
      - CONFIGURATION
      - CONTROL SYSTEMS
    - PROBLEMS
    - EQUATIONS OF MOTION
    - COARSE CONTROLLER
    - C.G. OFFSET EFFECT
    - RESULTS
      - PAYLOAD POINTING
      - MICRO-G
      - REBOOST
      - MRMS
  - FINE CONTROLLER
    - METHODS
    - CONTROL SYSTEM DEFINITION
    - STATUS & FUTURE ACTIVITIES
- CONCLUSIONS

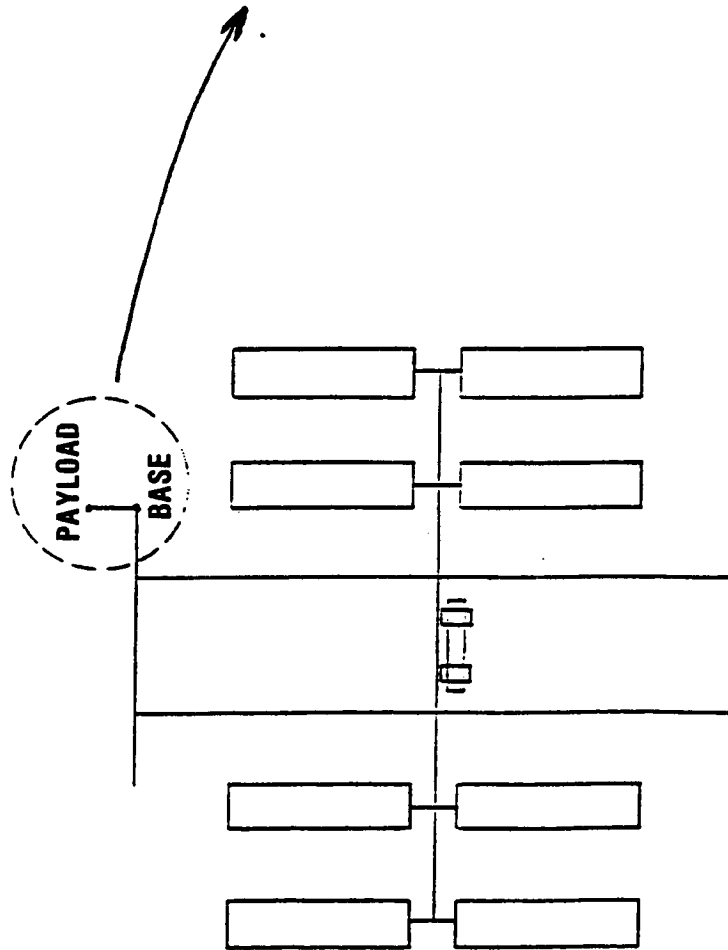
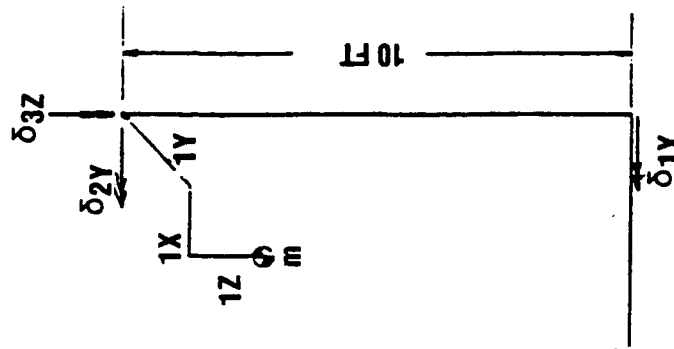


Rockwell International  
Space Station Systems Division

## CHART 3

A 9000 lb telescope with a 0.05 ft cg offset was chosen to represent a typical payload. The Space Station simulation model is shown in the figure. The telescope is attached to the top of the keel and its mass properties are listed. The model includes the control systems of the payload, alpha controller, the CMG controller, and the microgravity isolation controller.

# Telescope Used to Evaluate Pointing Problem



$I_X = I_Y = I_Z = .346\text{ M}$   
 $M = 275\text{ slug}$   
 $I_X = 1 \times 10^6\text{ slug} - \text{M}^2$   
 $I_Y = I_Z = 1.44 \times 10^7\text{ slug} - \text{IN}^2$

## CHART 4

The simulation model contains the listed modes. The 85 structural modes include 6 rigid body modes and 79 flexible modes. The other 8 control system modes are added to remove the locked constraint of the control surfaces (this constraint was used in the structural mode development). The 8 control surface modes are coupled with the structural modes so that the mass matrix is not diagonal.

The four control systems in the model are listed. The solar array pointing system and the CMG attitude pointing system have been modeled with position and rate feedback control. The magnetic isolation system for the migro-g experiment is one developed by Sperry and is a fifth order system for each of the translational degrees of freedom. The control system for the Coarse Pointing System (C.P.S) consists of a position and rate feedback system for the azimuth gimbal control, and position, rate and integral control for the elevation and cross elevation gimbal control.



# **Simulation Model Contains Coarse Pointing, Solar Array Control, Isolation and Vehicle Flexibility**

---



- **SIMULATION MODEL CONTAINS**
  - **Modes**
    - **85 STRUCTURAL MODES WITH LOCKED CONTROL JOINTS**
    - **3 ROTATIONAL COARSE POINTING MODES (C.P.S.)**
    - **2 ROTATIONAL SOLAR ARRAY MODES**
    - **3 TRANSLATIONAL MODES IN ISOLATION SYSTEM**
  - **CONTROLS**
    - **SOLAR ARRAY POINTING SYSTEM**
    - **ISOLATION CONTROL SYSTEM**
    - **CMG CONTROL SYSTEM**
    - **COARSE POINTING CONTROL SYSTEM**

## CHART 5

With the simulation model, the system stability is determined with the closed loop roots. Then the time response was calculated for the list of disturbances shown.

# Simulation Determines Stability and Transient Response

---



- RESULTS
- CLOSED-LOOP ROOTS
- TIME RESPONSE
- ALPHA COMMANDS
- CREW DISTURBANCE
- REBOOST
- MRMS



Rockwell International  
Space Station Systems Division

## CHART 6

The number of modes was limited to 85 because the mass matrix became ill-conditioned when more modes were used. The ill-conditioned mass matrix was caused by the rigid body modes that were added to remove the constraint at the alpha joints. Two potential solutions to solve this problem are: start with modes where the alpha joints have a spring instead of a lock or reduce the total degrees of freedom in the model.

# Numerical Problem May be Avoided by Modeling Alpha Joint Flexibility

---



- **PROBLEM**

- NUMERICAL INSTABILITY WHEN USING OVER 85 MODES DUE TO ILL-CONDITIONED MASS MATRIX

- **SOLUTION**

- OBTAIN MODES WITH SPRING AT ALPHA JOINT—THIS WILL RESULT IN RATE COUPLING & SHOULD REMOVE NUMERICAL PROBLEM
- REDUCE THE NUMBER OF SOLAR ARRAY DEGREES OF FREEDOM, THUS OBTAINING FEWER MODES FOR A GIVEN FREQUENCY RANGE

## CHART 7

The system equations are written in first order form. The first coefficient matrix shows the coupling between the rigid body modes for the control surfaces and the structural modes of the system. The coupling exist because these modes are not orthogonal to the structural modes of the system.

# System Equations Have Static, Rate, and Inertia Coupling



$$\begin{bmatrix} M_{ss} & M_{sp} & M_{sa} & M_{sq} \\ M_{ps} & M_{pp} & M_{pa} & M_{pq} \\ M_{as} & M_{ap} & M_{aa} & M_{aq} \\ M_{qs} & M_{qp} & M_{qa} & M_{qq} \end{bmatrix}
 \begin{bmatrix} \ddot{q}_s \\ \ddot{q}_p \\ \ddot{\alpha} \\ \ddot{\delta} \\ \ddot{q}_s \\ \ddot{q}_p \\ \ddot{\alpha} \\ \ddot{\delta} \\ \ddot{X}_p \\ \ddot{X}_s \end{bmatrix}
 +
 \begin{bmatrix} C_s + C_{cmg} & 0 & 0 & 0 & 0 & 0 & 0 & 0 & 0 & 0 \\ 0 & 0 & 0 & 0 & 0 & 0 & 0 & 0 & 0 & 0 \\ 0 & 0 & C_a & 0 & 0 & 0 & 0 & 0 & 0 & 0 \\ 0 & 0 & 0 & 0 & 0 & 0 & 0 & 0 & 0 & 0 \\ -1 & 0 & 0 & 0 & 0 & 0 & 0 & 0 & 0 & 0 \\ 0 & 0 & 0 & -1 & 0 & 0 & 0 & 0 & 0 & 0 \\ 0 & 0 & 0 & 0 & 0 & -1 & 0 & 0 & 0 & 0 \\ 0 & 0 & 0 & 0 & 0 & 0 & 0 & 0 & 0 & 0 \\ 0 & 0 & 0 & 0 & 0 & 0 & 0 & 0 & 0 & 0 \\ 0 & 0 & 0 & 0 & 0 & 0 & 0 & 0 & 0 & 0 \end{bmatrix}
 \begin{bmatrix} \dot{q}_s \\ \dot{q}_p \\ \dot{\alpha} \\ \dot{\delta} \\ q_s \\ q_p \\ \alpha \\ \delta \\ X_p \\ X_s \end{bmatrix}
 +
 \begin{bmatrix} K_s + K_{cmg} & 0 & 0 & 0 & 0 & 0 & 0 & 0 & 0 & 0 \\ 0 & 0 & 0 & 0 & 0 & 0 & 0 & 0 & 0 & 0 \\ 0 & 0 & K_a & 0 & 0 & 0 & 0 & 0 & 0 & 0 \\ 0 & 0 & 0 & K_a & 0 & 0 & 0 & 0 & 0 & 0 \\ 0 & 0 & 0 & 0 & K_{sq} & 0 & 0 & 0 & 0 & 0 \\ 0 & 0 & 0 & 0 & 0 & K_{sp} & 0 & 0 & 0 & 0 \\ 0 & 0 & 0 & 0 & 0 & 0 & K_{sa} & 0 & 0 & 0 \\ 0 & 0 & 0 & 0 & 0 & 0 & 0 & K_{sd} & 0 & 0 \\ 0 & 0 & 0 & 0 & 0 & 0 & 0 & 0 & -A & 0 \\ 0 & 0 & 0 & 0 & 0 & 0 & 0 & 0 & 0 & -K_{ss} \end{bmatrix}
 \begin{bmatrix} q_s \\ q_p \\ \alpha \\ \delta \\ X_p \\ X_s \end{bmatrix}$$

$$\begin{bmatrix} Q_s \\ 0 \\ Q_{\alpha C} \\ 0 \\ 0 \\ 0 \\ 0 \\ 0 \\ 0 \end{bmatrix}
 =
 \begin{bmatrix} a' \\ 0 \\ 0 \\ 0 \\ 0 \\ 0 \\ 0 \\ 0 \\ 0 \end{bmatrix}
 +
 \begin{bmatrix} 0 \\ 0 \\ K_{\alpha} \\ 0 \\ 0 \\ 0 \\ 0 \\ 0 \\ 0 \end{bmatrix}
 \alpha_C
 +
 \begin{bmatrix} 0 \\ 0 \\ C_{\alpha} \\ 0 \\ 0 \\ 0 \\ 0 \\ 0 \\ 0 \end{bmatrix}
 \dot{\alpha}_C$$

$q_s$  = RIGID + FLEXIBLE MODAL COORDINATES

$q_p$  = GAP IN ISOLATION SYSTEM

$\alpha$  = ALPHA ROTATION

$\delta$  = THREE ROTATIONAL D.O.F. ASSOCIATED WITH THE C.P.S.

$X_p$  = STATE VARIABLES ASSOCIATED WITH ISOLATION SYSTEM

$X\delta$  = STATE VARIABLES ASSOCIATED WITH C.P.S.

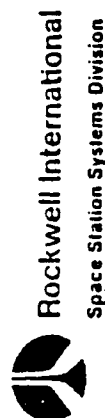


## CHART 8

The equations of motion are different when the modes are generated with a spring for the  $\alpha$  joint. The  $\alpha$  variable no longer appears explicitly in the equations. The coupling in the first coefficient matrix decreases but additional coupling appears in the second coefficient matrix. The new coupling results because  $\alpha$  is a function of the modal coordinates.



# System Equations With Alpha Spring in Modal Data



$$\begin{bmatrix} M_q & M_{sp} & M_{q\delta} & 0 & 0 & 0 & 0 & 0 \\ M_{ps} & M_p & 0 & 0 & 0 & 0 & 0 & 0 \\ M_{\delta q} & 0 & M_{\delta\delta} & 0 & 0 & 0 & 0 & 0 \\ 0 & 0 & 0 & 1 & 0 & 0 & 0 & 0 \\ 0 & 0 & 0 & 0 & 1 & 0 & 0 & 0 \\ 0 & 0 & 0 & 0 & 0 & 1 & 0 & 0 \\ 0 & 0 & 0 & 0 & 0 & 0 & 1 & 0 \\ 0 & 0 & 0 & 0 & 0 & 0 & 0 & 1 \end{bmatrix} \begin{Bmatrix} \ddot{q}_s \\ \ddot{q}_p \\ \ddot{\delta} \\ \dot{q}_s \\ \dot{q}_p \\ \dot{\delta} \\ \dot{x}_p \\ \dot{x}_\delta \end{Bmatrix} + \begin{Bmatrix} C_q + C_{cmg} + C_\alpha \Delta\theta_y^T \Delta\theta_y \\ 0 \\ \hat{C}_{\delta q} \\ -I \\ 0 \\ 0 \\ 0 \\ 0 \end{Bmatrix} \begin{Bmatrix} \dot{q}_s \\ \dot{q}_p \\ \dot{\delta} \\ q_s \\ q_p \\ \delta \\ x_p \\ x_\delta \end{Bmatrix} + \begin{Bmatrix} K_q + K_{cmg} \\ 0 \\ \hat{K}_{\delta q} \\ 0 \\ 0 \\ 0 \\ -K_{lq} \\ 0 \end{Bmatrix} \begin{Bmatrix} q_s \\ q_p \\ \delta \\ x_p \\ x_\delta \end{Bmatrix} = \begin{Bmatrix} a' \\ 0 \\ 0 \\ 0 \\ 0 \\ 0 \\ 0 \\ 0 \end{Bmatrix} + \begin{Bmatrix} f(t) + K_\alpha \\ 0 \\ 0 \\ 0 \\ 0 \\ 0 \\ 0 \\ 0 \end{Bmatrix} \begin{Bmatrix} \Delta\theta_y^T \\ 0 \\ 0 \\ 0 \\ 0 \\ 0 \\ 0 \\ 0 \end{Bmatrix} + \begin{Bmatrix} \Delta\theta_y^T \\ 0 \\ 0 \\ 0 \\ 0 \\ 0 \\ 0 \\ 0 \end{Bmatrix} \begin{Bmatrix} \alpha_c + C_\alpha \\ 0 \\ 0 \\ 0 \\ 0 \\ 0 \\ 0 \\ 0 \end{Bmatrix} + \begin{Bmatrix} \Delta\theta_y^T \\ 0 \\ 0 \\ 0 \\ 0 \\ 0 \\ 0 \\ 0 \end{Bmatrix} \begin{Bmatrix} \alpha_c \\ 0 \\ 0 \\ 0 \\ 0 \\ 0 \\ 0 \\ 0 \end{Bmatrix}$$

$\delta$  = THREE ROTATIONAL D.O.F. ASSOCIATED WITH THE C.P.S.  
 $x_p$  = STATE VARIABLES ASSOCIATED WITH ISOLATION SYSTEM  
 $x_\delta$  = STATE VARIABLES ASSOCIATED WITH C.P.S.  
 $q_s$  = RIGID + FLEXIBLE MODAL COORDINATES  
 $q_p$  = GAP IN ISOLATION SYSTEM

WHERE

## CHART 9

The payload C.G. could have a significant effect on the payload pointing error. The effect of this parameter may be evaluated without generating new modes. The mass matrix for a payload with a different C.G. offset is determined with the new sectionalized mass matrix and the previous set of modes.

# Effect of C.G. Offset May Be Obtained Without Generating New Modes

---



- A SIMULATION MODEL FOR PERFORMING PARAMETRIC STUDIES ON THE EFFECT OF C.G. OFFSET TERMS IN THE C.P.S. IS REQUIRED
- GENERATE NEW MASS MATRIX USING ASSUMED MODE METHOD
  - DEFINE NEW PAYLOAD C.G. OFFSET
  - GENERATE NASTRAN SECTIONALIZED MASS MATRIX [M]
  - ASSUME OLD MODES,  $[\phi] = \text{MODAL MATRIX}$
  - MULTIPLY  $[\phi]^T [M] [\phi] = [M]_{\text{NEW}}$

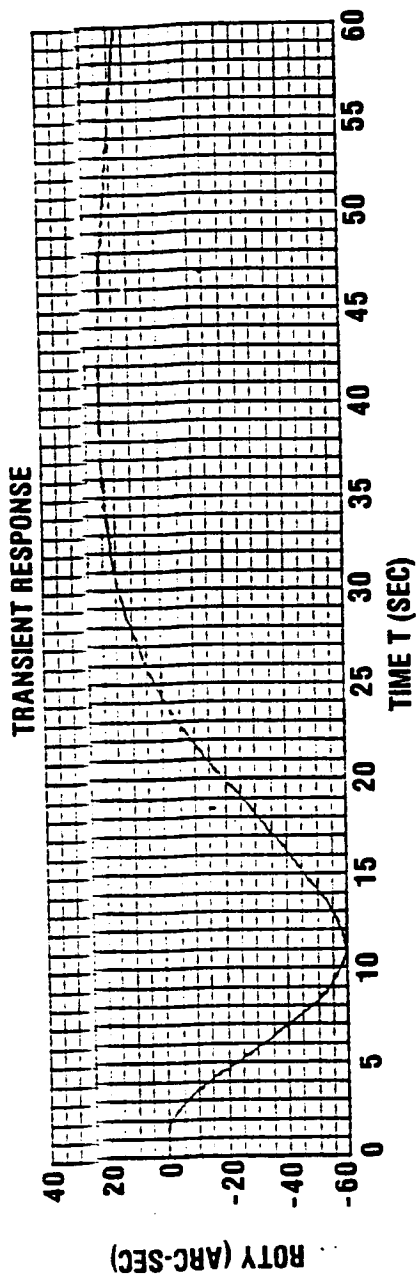


Rockwell International  
Space Station Systems Division

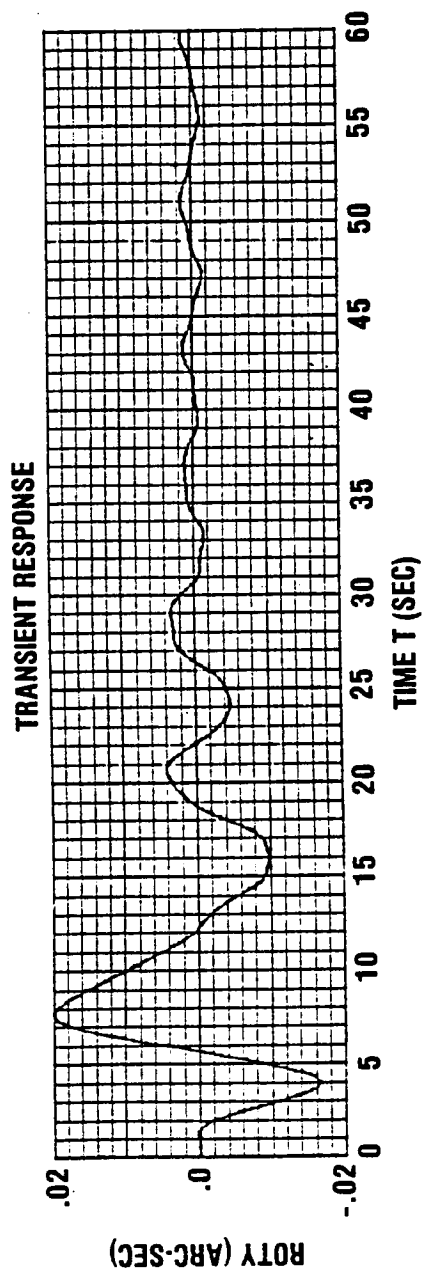
## CHART 10

The angular disturbance at the base of the payload has a maximum value of 60 arc-seconds. The disturbance in this case was a 2 degree command to the alpha controller. The command resulted in a torque near its capability. The response on the telescope is a maximum of 0.02 arc-seconds.

# Coarse-Pointing System Minimizes Pointing Error Due to Alpha Joint Rotation



Y--ROTATION AT BASE



Y--ROTATION AT PAYLOAD

$$\frac{\theta_P}{\theta_B} = \frac{.04}{59} = 7 \times 10^{-4}$$



Rockwell International  
Space Station Systems Division

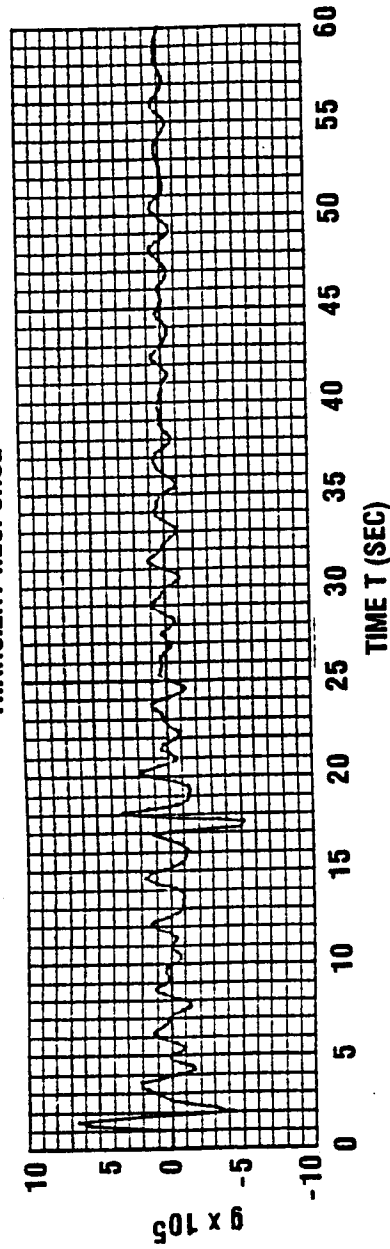
## CHART 11

The maximum acceleration at the base of the material processing experiment is  $6 \times 10^{-3}$ . The crew caused the disturbance by pushing off on one side of a module and stopping on the other side. The acceleration is reduced by the Sperry magnetic isolator to  $0.3 \times 10^{-3}$ .

# Isolator Reduces Crew Disturbance G-Level

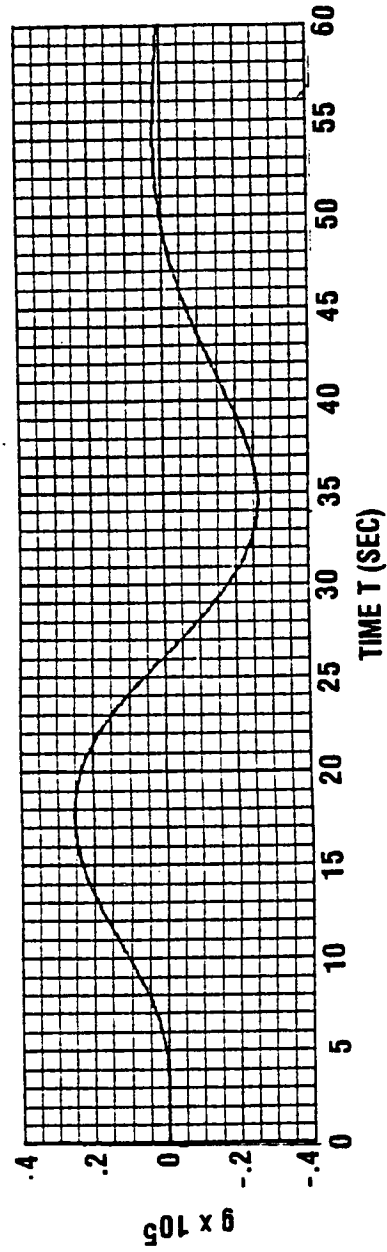


TRANSIENT RESPONSE



ACCELERATION LEVEL AT BASE

TRANSIENT RESPONSE



ACCELERATION LEVEL AT PAYLOAD

## CHART 12

The Sperry fine pointing control system being examined has 40 state variables. The translational and rotational isolation system is a electro magnetic isolation system and is mathematically similar to the micro-g isolation system.

C-6



# Fine-Pointing System Contains 40 State Variables

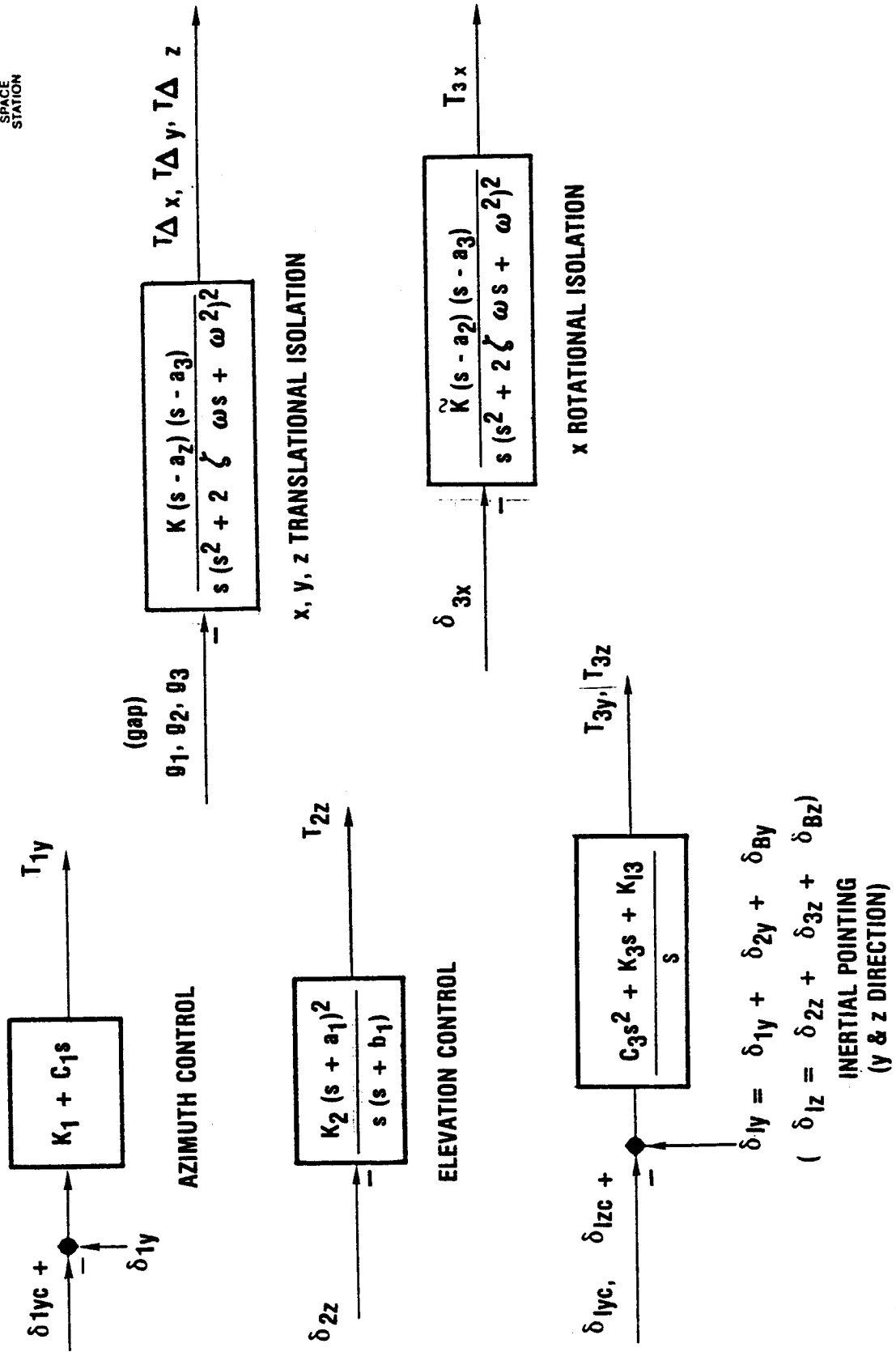


## CHART 13

A 203rd order simulation model was developed to evaluate the Space Station customer accommodation payload pointing and micro-g requirements. The simulation shows the pointing errors on the telescope are significantly smaller than at the base of the telescope. The pointing results could change when the parametric studies are performed. The results show the micro-g requirement is met with an active isolation system.

# Conclusions Payload Pointing and Microgravity

---



- SPACE STATION COARSE POINTING PROGRAM WITH 203rd ORDER SYSTEM & WITH 85 MODES (MAX. FREQ = 1.1 HZ) IS WORKING
- COARSE POINTING SYSTEM REDUCED ALPHA COMMAND DISTURBANCE FROM 60 ARC SEC AT BASE TO 0.02 ARC SEC
- MICRO-G REQUIREMENTS SATISFIED FOR CREW DISTURBANCE
- PARAMETRIC STUDY FOR DETERMINING C.G. OFFSET EFFECT MAY BE OBTAINED FROM CURRENT SIMULATION WITH MINOR MODIFICATIONS

Wednesday, April 23, 1986

SESSION 3

(Concurrent Sessions on Structures and Control)

Structures Session 3A - T. K. Hasselman, Chairman

SAFE Dynamic Flight Experiment	R. W. Schock, MSFC
Application of Robust Projection Operators to the Control of Flexible Structures with Uncertain Parameters	M. H. Bantell, Jr. Boeing
Dynamics of Trusses Having Nonlinear Joints	J. M. Chapman Boeing
Equivalent Beam Modeling Using Numerical Reduction Techniques	J. M. Chapman Boeing

Structures Session 3B - Wayne B. Holland, Chairman

Dynamic Characterization of a Vibrating Beam with Periodic Variation in Bending Stiffness	J. S. Townsend, MSFC
Structural Dynamic System Model Reduction	J. C. Chen, T. L. Rose, B. K. Wada, JPL
Space Telescope Reaction Wheel Assembly Vibration Damping System	R. E. Jewell, MSFC, P. Davis and J. Wilson, Sperry

PRECEDING PAGE BLANK NOT FILMED